

Alternative Indemnify More Effective Chemotherapy with Targeting Cancer Cell Using Encapsulation Technique

Marwa H. Mahmoud¹ , Shaimaa A. Gouhar^{2,*} 

¹ Department of Food Technology, National Research Centre, Dokki, Giza, Egypt

² Department of Medical Biochemistry, Medicine and Clinical Studies Research Institute, National Research Centre, Dokki, Giza, Egypt

* Corresponding author: ssadek007@gmail.com, ss.hashem@nrc.sci.eg

Scopus Author ID: 57214811089

Received: 31.10.2023; Accepted: 12.05.2024; Published: 25.08.2024

Abstract: Of all disorders, cancer ranks as one of the most fatal, causing up to 10 million fatalities in 2020. Chemotherapeutic drugs represent efficient therapy for a wide range of human cancers. The major obstacle in applying chemotherapy is the accompanying severe side effects. In the present study, nano-encapsulated bioactive compounds in the dietary supplements products with folate-targeting activity and pectin were designed to enhance the anticancer activity of two different formulas of nanoparticles: ND+F-dox (folic acid + doxorubicin in one capsule) and NDF-dox (folic acid, and doxorubicin in two separate capsules). Treatment of cancer cells with the two formulas significantly inhibited their proliferation in a concentration-dependent way with IC₅₀ values of 4.44, 36.15 µg/ml in the case of HepG2 cells and 2.36, 22.58 µg/ml in MCF-7 cells, respectively. The formulas had high selectivity by reporting very low toxicity with MCF10A normal cells. The anticancer effect of current formulas was due to a significant elevation of DNA damage as NDF-dox and ND+F-dox significantly increased percentages to 20.49, and 46.48%, respectively. The formulas significantly induced apoptosis by upregulating apoptotic BAX and downregulating anti-apoptotic Bcl2 simultaneously with high selectivity and specificity. The present research offers compelling proof that ND+F-dox succeeded in boosting the anticancer efficacy of doxorubicin and a successful prospective strategy to lessen doxorubicin toxicity by targeting cancer cells, increasing its application for cancer treatment.

Keywords: BCL-2; BAX; nano-encapsulated; doxorubicin; safe chemotherapy; alternative therapy.

© 2024 by the authors. This article is an open-access article distributed under the terms and conditions of the Creative Commons Attribution (CC BY) license (<https://creativecommons.org/licenses/by/4.0/>).

1. Introduction

Almost ten million cancer patients died globally in 2020, making it the top cause of death. In 2023, nearly 2 new million cancer cases and more than half a million cancer deaths occurred [1]. In the World Cancer Report 2020, breast cancer was the most predominant (2.26 million cases) [2]. Almost all human cancers are successfully treated with chemotherapy [3]. One of the most effective chemotherapeutic drugs is doxorubicin (dox), which is efficient against many cancers [4]. Unfortunately, dox is associated with negative side effects resulting from the widespread provision of free drugs without distinction [5,6]. So, focusing dox in tumor cells and decreasing its concentrations in normal tissues could improve the clinical application of dox by limiting its systemic toxicity. Nanotechnology can achieve such a goal as it has the potency to reduce chemotherapeutic toxicity by designing functionalized particles for targeted treatment [7,8].

Another way to minimize dox toxicity resulting from nonspecific systemic distribution of free drugs is the combinational use of multiple drugs, which provides many possible favorable outcomes for synergism, including low toxicity due to lower applied doses while maintaining high efficacy and low chances of drug resistance [9]. Pharmacological combinations are the most popular choice for treating chronic, incapacitating disorders [10,11]. The idea of a combination will be more favorable when the treatment plan includes chemotherapy and natural extract, which proves its potency as an anticancer agent. For a long time, natural extracts were employed widely in medicine. Several popular medications are made of natural substances or their derivatives. They have been reported as effective anticancer and anti-inflammatory agents [12,13]. Designing nanoparticles with a natural extract delivery system could strengthen their therapeutic efficacy. According to recent research, the bioavailability of natural compounds can be considerably increased by nanoparticles both in vitro and in vivo [14,15].

Of these natural extracts, pectin is an acidic heteropolysaccharide of plants and can be found in oranges or apples. Fruit pectin is important for gelling or thickening foods and stabilizing acid-based milk beverages. It has an advantage as a natural substance, as it can be ingested naturally. According to pectin's therapeutic effects and low toxicity, it has wide applications in the food and pharmaceutical industries [16]. Pectin has been reported as an anticancer agent in different cancer types, such as breast, head, and prostate cancer [17]. The anticancer effect of pectin is due to the anti-inflammatory properties induction of apoptosis through reducing the expression of anti-apoptotic Bcl2 protein expression with high selectivity to tumor cells, which is the greatest advantage of pectin over other synthetic anticancer medications [18,19]. In addition, pectin was demonstrated to have antioxidant and antibacterial activities [20,21]. Pectin is altered by a recently identified chemical mechanism, which releases pectin fragments throughout intestinal digestion. The resulting fragments adhere to and inhibit galectin 3 (Gal-3), preventing tumorigenesis [22].

Moreover, Vitamin E gained popularity in the late twentieth century as an anticancer substance through the control of the protein kinase C as well as of other kinases such as PI3K/Akt, ERK-MAPK, and cyclin-dependent kinases [23]. Also, Omega-3 fatty acids from fish oil bring many health benefits usable for cancer patients. In addition to their well-known anti-inflammatory effects, they have the potential to act synergistically with chemotherapy and increase tumor radiosensitivity [24]. A dietary supplement with a specific proportion of the previously mentioned natural constituents could control chronic diseases and associated complications [25]. Also, incorporating nano-encapsulated bioactive compounds in dietary supplements makes their handling easier for consumers, with the advantage of water-solubility properties, which guarantee high absorption and good bioavailability [26]. Thus, In the present study, we designed two different formulas of nanoparticles with pectin-folate-targeting activity to enhance the anticancer activity of doxorubicin while reducing its unfavorable side effects. Also, the formation of nano-encapsulated bioactive compounds for retarding cancer with a dietary supplement jelly form is our point of view.

2. Materials and Methods

2.1. Nano formulation of capsules.

Nanoencapsulation was done in accordance with Mahmoud *et al.* [26] with a few alterations:

2.1.1. W/O Nano-emulsion.

There were two prepared formulas for nano-emulsion. ND+F-dox: pectin, fish oil, and folic acid + doxorubicin (in one capsule). Second NDF-dox: pectin, fish oil, folic acid, and doxorubicin (in two separate capsules). W/O nano-emulsions were prepared by spontaneous emulsification. In short, a magnetic stirrer (VELP, Germany) was used to mix Span 80 and FA (folic acid) solution at 500 rpm (either alone or in conjunction with doxorubicin). The aqueous phase was then created by adding Span 80 dropwise to the fish oil phase while swirling magnetically at 1500 rpm: oil and a solution of surfactant made up the composition.

2.1.2. Biopolymer solution preparation.

To make 100 g of solutions, 2.5 g of pectin powder was dissolved in boiling deionized water. Concurrently, 10 g of WPC powder was dissolved in 45 ml of deionized water to create aqueous whey protein concentrate solutions. A magnetic stirrer was used to gently mix the solutions for at least thirty minutes. After mixing pectin and WPC solutions, the mixture was left overnight at room temperature to hydrate the biopolymers fully. The maltodextrin solution (75 ml) was added last.

2.1.3. W/O/W Nano-emulsion.

The W/O emulsion and biopolymer solution were combined and blended using a prop-ultrasonic (SONICS, Vibra-cell, VCX750, USA) and a high-speed homogenizer (CAT, Unidrive 1000 D, M. Zipperer GmbH, Germany) at a speed of 20,000 rpm.

2.1.4. Spray drying of emulsions.

A spray drier (B-290, Buchi) fitted with a pressure air atomizing nozzle at 2.5 bar air pressure, an intake air temperature of 180 °C, an exit air temperature of 90 °C, and a feed flow rate of 450 ml/h converted the produced emulsion solutions into encapsulated powder. Up to a subsequent examination, the dry powder was gathered and kept at 4 °C in dark, sealed containers.

2.2. Droplet size measurement.

With the use of a particle size analyzer (Nano-ZS, Malvern Instruments Ltd., UK), the samples' average diameter, size distribution, and zeta potential were determined. Before evaluation, the nanocapsule suspension was subjected to a 30- to 60-minute sonication cycle to measure its size distribution and zeta potential. Four measurements of each suspension were made using various refractive indices. A refractive index was employed to distinguish and describe each component separately for prepared capsules, including pectin, whey protein, doxorubicin, and folic acid.

2.3. Scanning electron microscopy of encapsulated powders.

Following the scattering of the nano-encapsulated powders over a two-sided sticky tape, a thin coating of gold was applied. Then, using a field emission scanning electron microscope (S-4160 Cold Field-Emission SEM, QUANTA, FEG 250, Thermo Fisher Scientific, USA) at an accelerated voltage of 320 kV, morphological characteristics of the particles were seen and photographed at 6000.

2.4. Fourier transforms infrared spectroscopy (FTIR).

Fourier transform infrared spectroscopy was used to analyze the materials' structural makeup (FT-IR). The materials' infrared spectra were captured using an FT-IR spectrophotometer manufactured by Shimadzu in Japan. Transmission mode was used to scan the spectrum between 400 and 4000 cm^{-1} of wavenumber. Prior to obtaining a spectrum, the dehydrated samples were combined with KBr powder and compressed into a disc.

2.5. Cell lines.

Human Hepatocellular carcinoma cell line (HepG2), breast carcinoma cells (MCF-7), and normal breast epithelial cells (MCF10A) were cultured in RPMI 1640 medium (Biowest), including 10% fetal bovine serum, L-glutamine (0.03%), penicillin (100 U/ml) and streptomycin (100 $\mu\text{g}/\text{ml}$). Cells were placed at 37°C with 5% CO_2 in a humidified environment. Adherent cells were seeded in a monolayer culture and regularly passaged with Trypsin/EDTA twice/week.

2.6. Cytotoxicity assay.

Cytotoxicity of doxorubicin, NDF-dox, and ND+F-dox were evaluated in HepG2, MCF-7, and MCF10A using 3 (4,5-dimethylthiazol-2-yl)-2,5-diphenyltetrazolium bromide (MTT) assay [27]. HepG2 and MCF-7 cells were cultured (1×10^4) in a 96-well plate for 24h. After that, Cells were exposed for 48h to different doses of the selected treatment options (final doses in the wells ranged from (3.125 -50 $\mu\text{g}/\text{ml}$) to assess the inhibitory effect for different extracts. After the treatment period, the cells were exposed to MTT for 4h, and the resulting formazan crystals were dissolved using ten percent SDS/0.01 M hydrochloric acid. The absorbance was read at 570 nm with reference to 690 nm.

$$\% \text{ viable cells} = \frac{(\text{absorbance of treated cells})}{(\text{absorbance of untreated cells})} \times 100$$

were utilized to investigate the IC50 values of the tested extracts, according to Yan and Caldwell [28].

2.7. DNA fragmentation.

DNA Fragmentation was used to measure the percent of degraded DNA after different treatments, according to Gibb and Gercel-Taylor [29]. After treatment of HepG2 and MCF-7 with 50% of IC50 doses of doxorubicin, ND+F-dox, and NDF-dox for 48 h, we collected all cell pellets then re-suspended in the lysis buffer and incubated for half an hour at 48°C. After that, tubes were centrifuged at 13,000 \times g for fifteen minutes at 4°C. Then, pellets were re-suspended in TE buffer and were precipitated by the addition of 25% Trichloroacetic Acid (TCA) and centrifugation at 500 \times g for 10min at 4°C, then the supernatant was discarded. Finally, tubes were heated at 100°C, cooled, and centrifuged at 300 \times g for fifteen minutes at 4°C. Degraded DNA was measured by diphenylamine (DPA) reagent.

$$\text{Percent of fragmented DNA} = \frac{\text{OD of supernatant}}{(\text{OD of supernatant} + \text{OD of pellet})} \times (2)$$

2.8. Quantitative RT-PCR.

Extraction and purification of RNA from cells was done by Qiagen's miRNeasy MiniKit (Hilden, Germany). The Revert Aid Reverse Transcriptase kit (Thermo Scientific) accomplished the reverse transcription of extracted RNA. Quantitect SYBR Green PCR reagents did real-time PCR on a Light Cycler Agilent Mx3000P, and the internal control GAPDH was used for normalization. Cycle thresholds (CTs) were measured, and fold changes were calculated using the $2^{-\Delta\Delta C_t}$ way. RT-PCR primers were provided by Qiagen: Bcl2 (Cat# QT00025011), BAX (Cat# QT00102536), and GAPDH (Cat# QT00079247).

2.9. Statistics.

The results were displayed as $m \pm sd$ after doing triplicate assays independently. To analyze the obtained data, we used one one-way ANOVA test and Tukey's multiple comparison test. Data is considered significant when $p < 0.05$.

3. Results and Discussion

3.1. Water/oil/water emulsion.

Emulsions are the potential new encapsulating and delivery technology for pharmaceuticals or bioactive chemicals. Their benefits have been highlighted, including controlled release and chemical stability of encapsulated substances. Doxorubicin nano-emulsion formation resulted in coordinating a W/O/W double emulsion by encasing the oil molecules around doxorubicin and/or folic acid in a WPC membrane. All of the molecules were then encased in yet another layer of pectin to generate a large molecule that encapsulates the small molecules inside, as illustrated in Figure 1. That structure allows more protection for its ingredients, as well as the protection of all body organs from doxorubicin hazards.

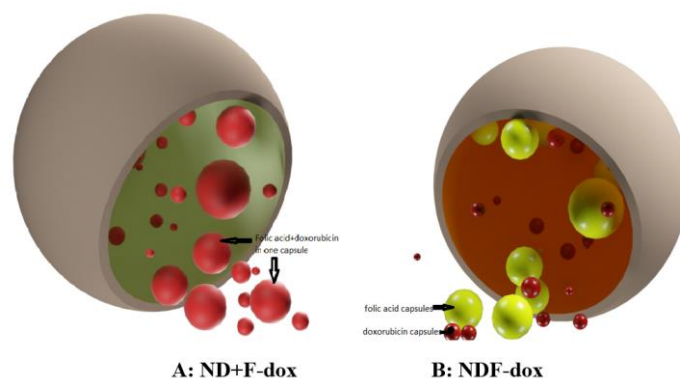


Figure 1. Nano-encapsulated doxorubicin (A) nano dox with folic acid in the same capsule; (B) nano dox in the capsule and folic acid in another capsule.

3.2. Encapsulated nano-doxorubicin with bioactive compound morphology by scanning electron microscopy SEM.

SEM was used to depict the shapes and sizes of formulated capsules. Figure 2 shows the microstructures of NDF-dox and ND+F-dox capsules. The WPC nanoparticles appeared in sizes ranging from 507–700 nm and made up the encapsulated powder. As illustrated in Figure 2, folic acid and doxorubicin particles were in the size 200-400 nm and 300-600 nm for both NDF-dox and ND+F-dox capsules, respectively. These particles are wrapped with a pectin layer to form particle sizes ranging from 900-2500 nm and 950-4000 nm for NDF-dox and

ND+F-dox, respectively. The surface pores of all capsules appeared in the SEM microstructure. NDF-dox and ND+F-dox had a more porous surface structure with hollow holes (Figure 2). This shape enabled high release and solubility, which were expected given the capsule's improved surface air permeability [30].

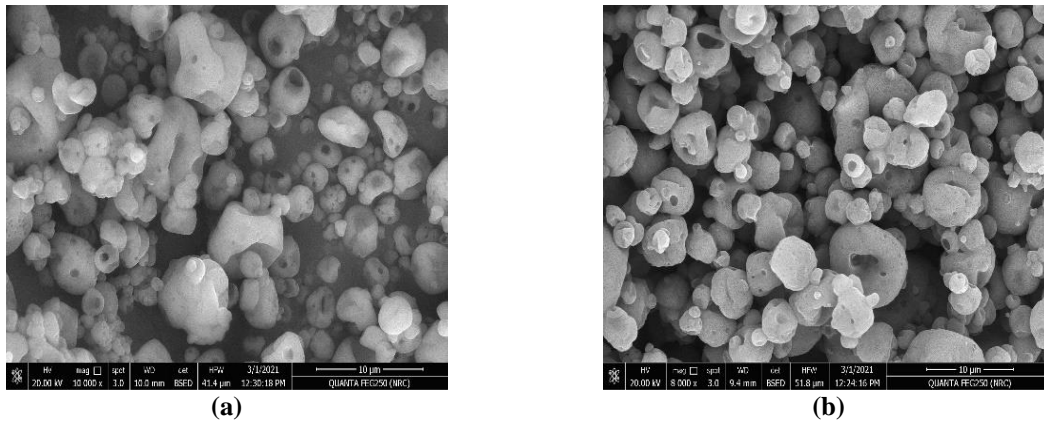


Figure 2. Scanning electron microscopy (SEM) images of (a) NDF-dox; (b) ND+F-dox.

3.3. Zeta size and potential of nano-pectin and nano-doxorubicin.

Bioavailability, stability, and solubility of oral administration of dietary supplement capsules could be predicted using the size and dispersion of particles. The size and distribution of the nanocapsules were measured using the dynamic light scattering (DLS) method, which is the most effective technique for examining the size distribution profile of materials suspended in solution [31]. Screening analysis of samples by DLS using the reflective index to differentiate the particles was applied. Results, as shown in Figure 2, indicate that all formulas of ND+F-dox capsules consisted of large particles wrapped with whey protein membrane; every large particle consisted of a number of small particles wrapped by pectin membrane. Nano-dox capsule (ND+F-dox) powder had a minuscule diameter of 344.5 nm (large capsule), while the small capsule consisted of doxorubicin + folic acid in one capsule at the diameter of 69.11 nm and 64.7 nm. On the other side, the Nano-dox capsule (NDF-dox) powder had a minuscule diameter of 485 nm (large capsule), while the small capsule consisted of doxorubicin and folic acid in two separate capsules at a diameter of 113.8 nm for folic acid and 54.23 nm for doxorubicin. Meanwhile, the particle size of doxorubicin powder without any treatments was 643.4 nm.

Although the physicochemical properties of powders may be modified by varying particle sizes, the encapsulated powders' finer and smaller particles can help increase their solubility and dispensability. To achieve acceptable stability, nanosuspensions must typically be electrostatically stabilized at a minimum zeta potential of 30 mV. Additionally, in the event of the interaction of the steric and electrostatic forces, 20 mV of zeta potential is enough. This is due to the fact that the hydrophilic surfactant coat can increase the emulsion's stability by further hydrating the surface layer [32]. The treated samples' zeta potentials had a strong negative charge of 51.03 and 48.28 for ND+F-dox and NDF-dox, respectively. This suggests that the sample of nanocapsules showed greater stability in aqueous dispersion. This demonstrates that it was thought the nano-loaded polymer system would be stable. These results were consistent with those of Guo *et al.* [33], who showed that polysaccharides, such as pectin and soybean soluble polysaccharides (SSPs), are difficult to establish a stable colloidal or emulsion system other than at the electro-kinetic potential. Polysaccharides also

have a propensity to coagulate or flocculate. Also, Dox-loaded polymer capsules had a lot of surface area because polymer molecules were trapped inside them, which may be why the negative charge on the capsules' surfaces was amplified.

3.4. Characterization of encapsulated powder by FTIR.

Upon comparing the FT-IR spectra of pectin that had been treated, significant functional groups that had been found were observed, therefore validating crucial aspects of the pectin configuration. The bands in the range of 800-1300 cm^{-1} are known as the "footprint of the pectin molecule" region, conjugated C-C double bonds. FTIR spectrum showed the characteristic peaks of doxorubicin: at 835 cm^{-1} , 952 cm^{-1} , and 1309 cm^{-1} , the bending vibrations of the amino group. The main absorption peaks of NDF-dox and ND+F-dox were in 1789, 1764, 1618, and 1309 cm^{-1} .

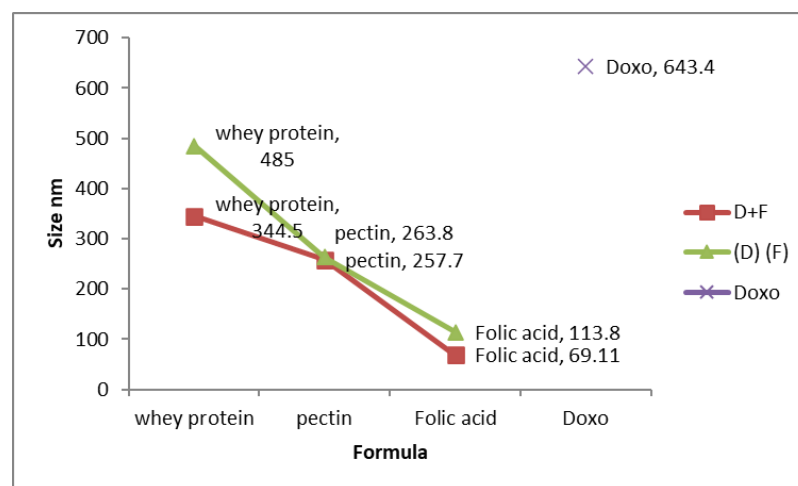


Figure 3. Zeta size distribution of formulas.

A non-destructive method for examining the functional groups in food matrices is the FTIR method. Figure 4 shows the FTIR spectra of NDF-dox and ND+F-dox with whey protein, pectin, and maltodextrin (3). The peak shows the double bond of an omega-3 unsaturated fatty acid at 2400 cm^{-1} , which is present in all samples.

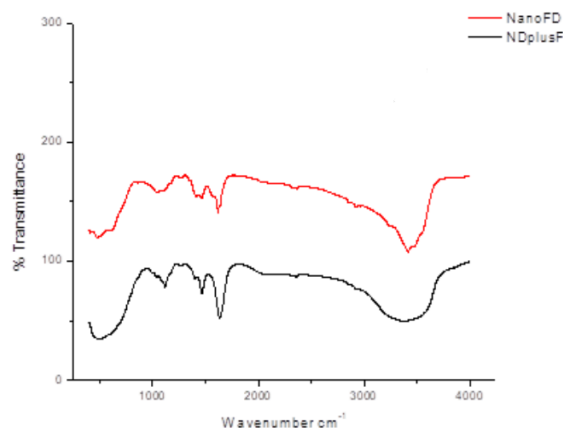


Figure 4. FTIR spectrum of NDF-dox, ND+F-dox.

The peaks at 2925 and 2856 cm^{-1} , on the other hand, are indicative of the hydrocarbon's alkene and alkane stretch vibrations. In NDF-dox and ND+F-dox, the strength of these peaks

was higher. The FTIR spectra of the capsules show two peaks at 3635 and 1554 cm^{-1} , which are ascribed to the amide's asymmetric N-H ($-\text{NH}^{3+}$) and O-H stretching. The whey protein's secondary structure's α -helix was shown by the amide peak at 1816 cm^{-1} [34] (Dybing & Smith, 1991). Additionally, the primary component of whey protein is β -lactoglobulin (apex 57%), which gives their amphiphilic molecules emulsifying qualities that can improve emulsion stability, produce desired emulsion characteristics, and lessen the interfacial tension between the hydrophilic and lipophilic phases. The peak shows the carbonyl stretching group of the triacylglycerols in unsaturated fatty acids at 2408 cm^{-1} .

3.5. Cytotoxicity assay.

the anticancer effect of doxorubicin, ND+F-dox, and NDF-dox was investigated in HepG2, MCF-7 and MCF10A normal cells. Cells without treatment were regarded as controls (cell viability=100%). The viability of the HepG2 and MCF-7 cells decreased gradually with the increase in drug concentrations. It can be observed that all drugs showed concentration-dependent cytotoxicity (Figure 5). IC50 values were calculated and listed in Table 1. In the case of HepG2 cells, the IC50 values of dox, ND+F-dox, and NDF-dox were 8.71, 4.44, and 36.15 $\mu\text{g/ml}$, respectively while they were 5.59, 2.36, and 22.58 $\mu\text{g/ml}$ respectively in case of MCF-7 cells. Regarding the normal breast cell model MCF10A cells, dox showed significantly high toxicity (IC50:79.39 $\mu\text{g/ml}$) while the 2 formulas ND+F-dox and NDF-dox showed very low toxicity (IC50:123.52 and 136.85 $\mu\text{g/ml}$ respectively). It was investigated that dox and the two formulas were able to inhibit cell growth significantly, where ND+F-dox was the best to inhibit cancer cell proliferation by recording the least IC50 in both cancer cell lines. Results indicated a high significant difference ($p < 0.001$) between all groups compared to control untreated HepG2 and MCF7 cells. The specificity of our designed nano formulas against tumor cells is highly important for clinical applications and validates its efficacy as a chemopreventive or anticancer agent. The ability to accurately differentiate between cancer and normal cells is another obstacle for any anticancer agent. Current data showed the significantly low cytotoxic effect of the two formulas on MCF10A normal cells when compared to MCF7 and HepG2 cancer cells, ensuring high specificity of ND+F-dox and NDF-dox. This specific delivery may be due to folic acid, which allows tumor cell endocytosis by identifying its counterpart, which is highly found in the tumor cell surface [35]. This provides a healthier method for targeting cancer, as Cheng *et al.* [36] and Ditto *et al.* [37] reported. Also, Scomparin *et al.* [38] recorded similar results for folic acid-modified doxorubicin nanoparticles showing a specific target to cancer cells. Furthermore, the oil layer surrounding nanoparticles in our study was covered by another layer of pectin, which may contribute to lower toxicity against normal cells. This agrees with Yu *et al.* [39], who reported that Pectin-doxorubicin conjugated macromolecule nanoparticles showed a long half-life, good hydrophilicity, and low toxicity compared to dox.

Table 1. IC50 values of different formulas in treated MCF7 and HepG2 cell lines.

Drug	Cell line		
	MCF10A	MCF7	HepG2
Dox	4.21***	5.59***	8.71***
ND+F-dox	79.39	2.36***	4.44***
NDF-dox	123.52	22.58**	36.15**

** $p < 0.01$, *** $p < 0.001$.

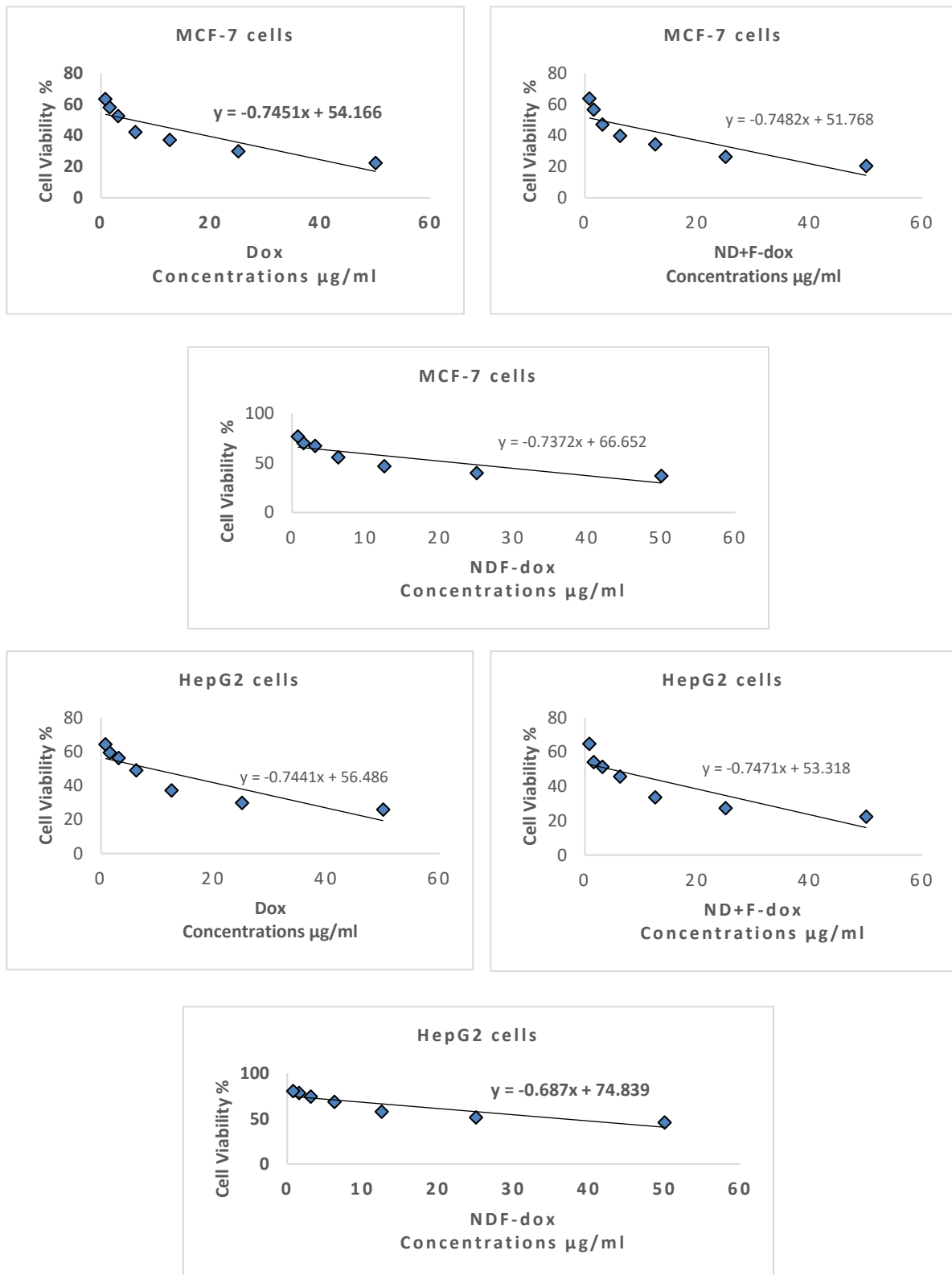


Figure 5. Cytotoxic effect of different formulas on the viability of MCF7 and HepG2 cells.

3.6. DNA fragmentation.

To further evaluate whether induced cell death by the two formulas was accompanied by nuclear DNA damage or apoptosis induction. The percentage of DNA fragmentation after exposure to doxorubicin, ND+F-dox, and NDF-dox revealed that all used drugs have a significant effect on DNA damage, as NDF-dox significantly elevated DNA damage

percentages to 20.49%; however, doxorubicin and ND+F-dox, showed tremendous increase in the percentage of fragmented DNA to reach 41.91% and 46.48% (Figure 6A). Based on these results, the cancer cell death in our study is accompanied by DNA fragmentation, which is an indication of apoptosis in which the chromosomal DNA is cleaved into oligo nucleosome-sized fragments as an integral part of apoptosis [9,40,41]. Due to its evident role in mediating cell death in response to cancer chemotherapy and radiation, apoptosis has recently attracted much attention [42,43]. The high focus on apoptosis was also due to the discovery of many genes that can regulate cell apoptotic processes [44].

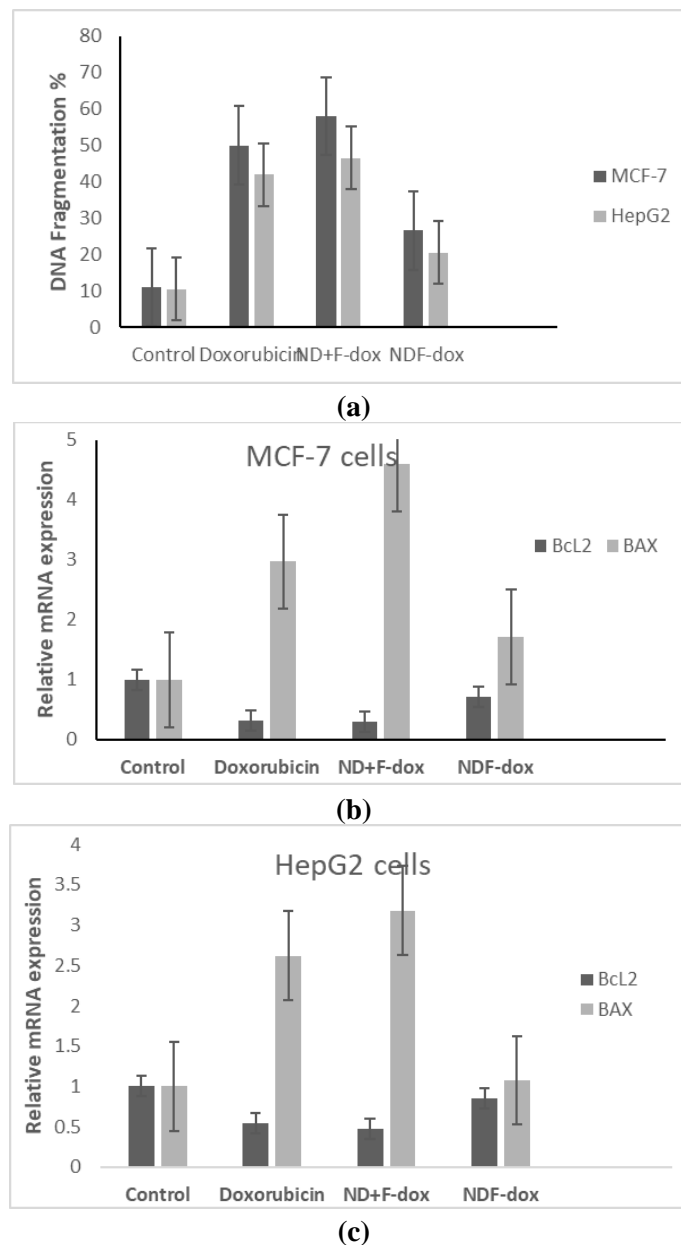


Figure 6. Mechanism of action of different formulas on MCF7 and HepG2 cells. (a) DNA fragmentation ratio of cells after 48h treatment; (b) mRNA expression of Bcl2 and BAX in MCF7 cells after 48h treatment; (c) mRNA expression of Bcl2 and BAX in HepG2 cells after 48h treatment.

3.7. The Expression of the Apoptotic Marker Bcl-2 and Anti-Apoptotic Marker BAX attractive targets in cancer therapy.

Identifying the mechanisms of apoptosis induction in cancer cells will greatly affect cancer treatment. To further unveil the molecular mechanism of apoptosis enhancement by the drugs, the expression of the apoptotic key effector B cell lymphoma-2 (Bcl-2), as well as the <https://nanobioletters.com/>

anti-apoptotic marker BAX, was evaluated as they are important components of the apoptosis process [45]. The pro-apoptotic BAX and BAK have the ability to obligate cells to apoptosis by increasing the permeability of the mitochondrial membrane and initiating caspases, while anti-apoptotic Bcl-2 was found to facilitate oncogenesis through cell death resistance [46,47]. In the current research, the Bcl-2 was significantly downregulated while pro-apoptotic BAX was upregulated in a significant way after exposing cells to dox and ND+F-dox (Figure 6B, C), which ensures the induction of apoptosis after different treatments used in the current study.

4. Conclusions

The previous results show that ND+F-dox is the best formula for anticancer effect and specificity. Its efficacy is significantly higher than that of dox and the other formulas. It is well documented that dox is associated with harmful effects involving the heart and liver due to its high toxicity and low selectivity. As an alternative, ND+F-dox could decrease these harmful effects of chemotherapy through the sustained release of anticancer drugs and active targeting with high selectivity towards cancer cells. The difference in design between NDF-dox and ND+F-dox may be the cause of the difference in efficacy. The presence of dox in the same capsule with pectin, fish oil, and folic acid decreased the efficacy of dox significantly; however, it is still a good anticancer agent with high specificity. The research presented here offers convincing proof that ND+F-dox can improve the efficacy of dox, resulting in a significant antiproliferative effect initiation of the apoptotic pathway with high specificity. This formula could be a successful potential mitigation strategy to decrease the undesired effects of dox by targeting cancer cells, therefore increasing its clinical application.

Funding

The work was funded by the National Research Centre as a part of a project (grantee No: 12010407/ 2019-2021) to allow for the potentiality to complete this research as a part of this project.

Acknowledgments

The authors would like to express their deepest gratefulness to the National Research Centre for the kind assistance in completing this work as a part of a project (grantee No: 12010407/2019-2021).

Conflicts of Interest

The authors declare no conflict of interest.

References

1. Siegel, R.L.; Miller, K.D.; Wagle, N.S.; Jemal, A. Cancer statistics, 2023. *CA Cancer J. Clin.* **2023**, *73*, 17-48, <http://doi.org/10.3322/caac.21763>.
2. Connal, S.; Cameron, J.M.; Sala, A.; Brennan, P.M.; Palmer, D.S.; Palmer, J.D.; Perlow, H.; Baker, M.J. Liquid biopsies: the future of cancer early detection. *J. Transl. Med.* **2023**, *21*, 118, <http://doi.org/10.1186/s12967-023-03960-8>.
3. Behranvand, N.; Nasri, F.; Zolfaghari Emameh, R.; Khani, P.; Hosseini, A.; Garssen, J.; Falak, R. Chemotherapy: a double-edged sword in cancer treatment. *Cancer Immunol. Immunother.* **2022**, *71*, 507-526, <https://doi.org/10.1007/s00262-021-03013-3>.
4. Kanwal, U.; Irfan Bukhari, N.; Ovais, M.; Abass, N.; Hussain, K.; Raza, A. Advances in nano-delivery <https://nanobioletters.com/>

- systems for doxorubicin: an updated insight. *J. Drug Target.* **2018**, *26*, 296-310, <https://doi.org/10.1080/1061186X.2017.1380655>.
5. Dulf, P.L.; Mocan, M.; Coadă, C.A.; Dulf, D.V.; Moldovan, R.; Baldea, I.; Farcas, A.-D.; Blendea, D.; Filip, A.G. Doxorubicin-induced acute cardiotoxicity is associated with increased oxidative stress, autophagy, and inflammation in a murine model. *Naunyn Schmiedebergs Arch. Pharmacol.* **2023**, *396*, 1105-1115, <https://doi.org/10.1007/s00210-023-02382-z>.
 6. Park, J.; Fong, P.M.; Lu, J.; Russell, K.S.; Booth, C.J.; Saltzman, W.M.; Fahmy, T.M. PEGylated PLGA nanoparticles for the improved delivery of doxorubicin. *Nanomed.: Nanotechnol. Biol. Med.* **2009**, *5*, 410-418, <http://doi.org/10.1016/j.nano.2009.02.002>.
 7. Mokhtar, N.; Fouda, F.; Zaazaa, A.M.; Mahmoud, M.H. Nano-Encapsulation of Doxorubicin Using Pectin: Safety and Activity on Chemotherapy-Induced Cardiotoxicity in Carcinoma Mice. *Lett. Appl. NanoBioSci.* **2023**, *12*, 107, <https://doi.org/10.33263/LIANBS124.107>.
 8. Mosleh-Shirazi, S.; Abbasi, M.; Reza Moaddeli, M.; Vaez, A.; Shafiee, M.; Kasaei, S.R.; Amani, A.M.; Hatam, S. Nanotechnology advances in the detection and treatment of cancer: an overview. *Nanotheranostics* **2022**, *6*, 400, <https://doi.org/10.7150/ntno.74613>.
 9. El-Daly, S.M.; Gouhar, S.A.; Gamal-Eldeen, A.M.; Abdel Hamid, F.F.; Ashour, M.N.; Hassan, N.S. Synergistic effect of α -solanine and cisplatin induces apoptosis and enhances cell cycle arrest in human hepatocellular carcinoma cells. *Anti-Cancer Agents Med. Chem.* **2019**, *19*, 2197-2210, <https://doi.org/10.2174/1871520619666190930123520>.
 10. Elshahid, Z.A.; Salama, A.; Gouhar, S.A. Assessment of the synergistic anti-inflammatory effect of naringin/sulindac for the treatment of osteoarthritis: in vitro and in vivo. *Adv. Tradit. Med.* **2024**, *24*, 265-283, <https://doi.org/10.1007/s13596-023-00692-4>.
 11. Mokhtari, R.B.; Homayouni, T.S.; Baluch, N.; Morgatskaya, E.; Kumar, S.; Das, B.; Yeager, H. Combination therapy in combating cancer. *Oncotarget* **2017**, *8*, 38022, <https://doi.org/10.18632/oncotarget.16723>.
 12. Salama, A.; Sadek, S.A.; El Shahed, Z.A.E. Naringin Attenuates D-galactose-Induced Brain Aging Via Regulation Of Oxidative Stress Markers TNF- α , NF- κ B And Modulation Of The Neurotrophic Markers PGC1- α , NT-3 AGEs, And GFAP In Vivo. *Egypt. J. Chem.* **2024**, *67*, 1-15, <https://doi.org/10.21608/ejchem.2023.212559.8002>.
 13. El-Daly, S.M.; Gamal-Eldeen, A.M.; Gouhar, S.A.; Abo-elfadl, M.T.; El-Saeed, G. Modulatory Effect of Indoles on the Expression of miRNAs Regulating G1/S Cell Cycle Phase in Breast Cancer Cells. *Appl. Biochem. Biotechnol.* **2020**, *192*, 1208-1223, <https://doi.org/10.1007/s12010-020-03378-8>.
 14. Sachdeva, A.; Dhawan, D.; Jain, G.K.; Yerer, M.B.; Collignon, T.E.; Tewari, D.; Bishayee, A. Novel Strategies for the Bioavailability Augmentation and Efficacy Improvement of Natural Products in Oral Cancer. *Cancers* **2023**, *15*, 268, <https://doi.org/10.3390/cancers15010268>.
 15. Watkins, R.; Wu, L.; Zhang, C.; Davis, R.M.; Xu, B. Natural product-based nanomedicine: recent advances and issues. *Int. J. Nanomed.* **2015**, *10*, 6055-6074, <https://doi.org/10.2147/ijn.s92162>.
 16. Virginia Rodríguez, R.; Lucía Isabel Castro, V. Pectin - Extraction, Purification, Characterization and Applications. In *Pectins*, Martin, M., Ed.; IntechOpen, Rijeka, **2019**; Ch. 3, <http://doi.org/10.5772/intechopen.85588>.
 17. Sharma, N.; Rathore, M.; Sharma, M. Microbial pectinase: sources, characterization and applications. *Rev. Environ. Sci. Biotechnol.* **2013**, *12*, 45-60, <https://doi.org/10.1007/s11157-012-9276-9>.
 18. Delphi, L.; Sepehri, H.; Khorramizadeh, M.R.; Mansoori, F. Pectic-Oligosaccharides from Apples Induce Apoptosis and Cell Cycle Arrest in MDA-MB-231 Cells, a Model of Human Breast Cancer. *Asian Pac. J. Cancer Prev. APJCP* **2015**, *16*, 5265-5271, <http://doi.org/10.7314/apjcp.2015.16.13.5265>.
 19. Hosseini Abari, A.; Amini Rourani, H.; Ghasemi, S.M.; Kim, H.; Kim, Y.-G. Investigation of antioxidant and anticancer activities of unsaturated oligo-galacturonic acids produced by pectinase of *Streptomyces hydrogenans* YAM1. *Sci. Rep.* **2021**, *11*, 8491, <http://doi.org/10.1038/s41598-021-87804-9>.
 20. Mahmoud, M.H.; Abu-Salem, F.M.; Azab, D.E.-S.H. A Comparative Study of Pectin Green Extraction Methods from Apple Waste: Characterization and Functional Properties. *Int. J. Food Sci.* **2022**, *2022*, 2865921, <https://doi.org/10.1155/2022/2865921>.
 21. Hassan, E.; Fadel, S.; Abou-Elseoud, W.; Mahmoud, M.; Hassan, M. Cellulose Nanofibers/Pectin/Pomegranate Extract Nanocomposite as Antibacterial and Antioxidant Films and Coating for Paper. *Polymers* **2022**, *14*, 4605, <https://doi.org/10.3390/polym14214605>.
 22. Emran, T.B.; Islam, F.; Mitra, S.; Paul, S.; Nath, N.; Khan, Z.; Das, R.; Chandran, D.; Sharma, R.; Lima, C.M.; Awadh, A.A.; Almazni, I.A.; Alhasaniah, A.H.; Guiné, R.P.F. Pectin: A Bioactive Food Polysaccharide

- with Cancer Preventive Potential. *Molecules* **2022**, *27*, 7405, <https://doi.org/10.3390/molecules27217405>.
23. Mutalip, S.S.M. Vitamin E: Nature's Gift to Fight Cancer. In *Anticancer plants: Properties and Application: Volume 1*, Akhtar, M.S., Swamy, M.K., Eds.; Springer Singapore, Singapore, **2018**; pp. 367-393. https://doi.org/10.1007/978-981-10-8548-2_16.
 24. Neuwirthová, J.; Gál, B.; Smilek, P.; Urbánková, P.; Kostřica, R. Anticancer Effect of Fish Oil—a Fable or the Truth?. *Klinická Onkologie: Casopis Ceske a Slovenske Onkologicke Spolecnosti* **2016**, *29*, 100-106, <https://doi.org/10.14735/amko2016100>.
 25. El-Shobaki, F.A.; Maha, H.M.; Badawy, I.H.; Marwa, H.M. A dietary supplement to Ameliorate Hyperglycemia and associated complications in Streptozotocin injected rats. *Int. J. Chemtech Res.* **2015**, *8*, 399-410.
 26. Mahmoud, M.H.; Mehaya, f.m.; abu-salem, f.m. ENCAPSULATION OF POMEGRANATE SEED OIL USING W/O/W NANO-EMULSION TECHNIQUE FOLLOWED BY SPRAY DRYING AND ITS APPLICATION IN JELLY FORM. *J. Microbiol. Biotechnol. Food Sci.* **2020**, *10*, 449-453, <https://doi.org/10.15414/jmbfs.2020.10.3.449-453>.
 27. Hansen, M.B.; Nielsen, S.E.; Berg, K. Re-examination and further development of a precise and rapid dye method for measuring cell growth/cell kill. *J. Immunol. Methods* **1989**, *119*, 203-210, [https://doi.org/10.1016/0022-1759\(89\)90397-9](https://doi.org/10.1016/0022-1759(89)90397-9).
 28. Yan, Z.; Caldwell, G.W. Evaluation of Cytochrome P450 Inhibition in Human Liver Microsomes. In *Optimization in Drug Discovery: In Vitro Methods*, Yan, Z., Caldwell, G.W., Eds.; Humana Press, Totowa, NJ, **2004**; pp. 231-244, <https://doi.org/10.1385/1-59259-800-5:231>.
 29. Gibb, R.K.; Gercel-Taylor, C. Use of Diphenylamine in the Detection of Apoptosis. In *Ovarian Cancer: Methods and Protocols*, Bartlett, J.M.S., Ed.; Humana Press: Totowa, NJ, **2001**; 679-680, <https://doi.org/10.1385/1-59259-071-3:679>.
 30. Mahdavee Khazaei, K.; Jafari, S.M.; Ghorbani, M.; Hemmati Kakhki, A. Application of maltodextrin and gum Arabic in microencapsulation of saffron petal's anthocyanins and evaluating their storage stability and color. *Carbohydr. Polym.* **2014**, *105*, 57-62, <http://doi.org/10.1016/j.carbpol.2014.01.042>.
 31. Khazaei, K.M.; Jafari, S.M.; Ghorbani, M.; Kakhki, A.H.; Sarfarazi, M. Optimization of Anthocyanin Extraction from Saffron Petals with Response Surface Methodology. *Food Anal. Methods* **2016**, *9*, 1993-2001, <http://doi.org/10.1007/s12161-015-0375-4>.
 32. Tamjidi, F.; Shahedi, M.; Varshosaz, J.; Nasirpour, A. EDTA and α -tocopherol improve the chemical stability of astaxanthin loaded into nanostructured lipid carriers. *Eur. J. Lipid Sci. Technol.* **2014**, *116*, 968-977, <https://doi.org/10.1002/ejlt.201300509>.
 33. Guo, X.; Zhao, W.; Pang, X.; Liao, X.; Hu, X.; Wu, X. Emulsion stabilizing properties of pectins extracted by high hydrostatic pressure, high-speed shearing homogenization and traditional thermal methods: A comparative study, *Food Hydrocoll.* **2014**, *35*, 217–225, doi: 10.1016/j.foodhyd.2013.05.010.
 34. Dybing, S.T.; Smith, D.E. Relation of chemistry and processing procedures to whey protein functionality: a review, *Dairy Prod. J.* **1991**, *26*, 4–12.
 35. Ibrahim, M.A.I.; Othman, R.; Chee, C.F.; Ahmad Fisol, F. Evaluation of Folate-Functionalized Nanoparticle Drug Delivery Systems—Effectiveness and Concerns. *Biomedicines* **2023**, *11*, 2080, <https://doi.org/10.3390/biomedicines11072080>.
 36. Cheng, W.; Nie, J.; Xu, L.; Liang, C.; Peng, Y.; Liu, G.; Wang, T.; Mei, L.; Huang, L.; Zeng, X. pH-Sensitive Delivery Vehicle Based on Folic Acid-Conjugated Polydopamine-Modified Mesoporous Silica Nanoparticles for Targeted Cancer Therapy. *ACS Appl. Mater. Interfaces* **2017**, *9*, 18462-18473, <http://doi.org/10.1021/acsami.7b02457>.
 37. Ditto, A.J.; Shah, K.N.; Robishaw, N.K.; Panzner, M.J.; Youngs, W.J.; Yun, Y.H. The Interactions between l-Tyrosine Based Nanoparticles Decorated with Folic Acid and Cervical Cancer Cells under Physiological Flow. *Mol. Pharmaceutics* **2012**, *9*, 3089-3098, <http://doi.org/10.1021/mp300221f>.
 38. Scomparin, A.; Salmaso, S.; Eldar-Boock, A.; Ben-Shushan, D.; Ferber, S.; Tiram, G.; Shmeeda, H.; Landa-Rouben, N.; Leor, J.; Caliceti, P.; Gabizon, A.; Satchi-Fainaro, R. A comparative study of folate receptor-targeted doxorubicin delivery systems: Dosing regimens and therapeutic index. *J. Control. Release* **2015**, *208*, 106-120, <http://doi.org/10.1016/j.jconrel.2015.04.009>.
 39. Yu, C.-y.; Yang, S.; Li, Z.-p.; Huang, C.; Ning, Q.; Huang, W.; Yang, W.-t.; He, D.; Sun, L. The In-Situ One-Step Synthesis of a PDC Macromolecular Pro-Drug and the Fabrication of a Novel Core-Shell Micell. *Curr. Pharm. Des.* **2016**, *22*, 506-513, <http://doi.org/10.2174/1381612822888151207095620>.
 40. Zhang, J.; Xu, M. Apoptotic DNA fragmentation and tissue homeostasis. *Trends Cell Biol.* **2002**, *12*, 84-89,

- [https://doi.org/10.1016/s0962-8924\(01\)02206-1](https://doi.org/10.1016/s0962-8924(01)02206-1).
41. Salam, S.G.A.; Rashed, M.M.; Ibrahim, N.A.; Rahim, E.A.A.; Alsufiani, H.M.; Mansouri, R.A.; Afifi, M.; Al-Farga, A. Cell Growth Inhibition, DNA Fragmentation and Apoptosis-Inducing Properties of Household-Processed Leaves and Seeds of Fenugreek (*Trigonella Foenum-Graecum* Linn.) against HepG2, HCT-116, and MCF-7 Cancerous Cell Lines. *Curr. Issues Mol. Biol.* **2023**, *45*, 936-953, <https://doi.org/10.3390/cimb45020060>.
 42. Gouhar, S.A.; Abo-elfadl, M.T.; Gamal-Eldeen, A.M.; El-Daly, S.M. Involvement of miRNAs in response to oxidative stress induced by the steroidal glycoalkaloid α -solanine in hepatocellular carcinoma cells. *Environ. Toxicol.* **2022**, *37*, 212-223, <https://doi.org/10.1002/tox.23390>.
 43. Xu, X.; Lai, Y.; Hua, Z.-C. Apoptosis and apoptotic body: disease message and therapeutic target potentials. *Biosci. Rep.* **2019**, *39*, BSR20180992, <https://doi.org/10.1042/BSR20180992>.
 44. Kiraz, Y.; Adan, A.; Kartal Yandim, M.; Baran, Y. Major apoptotic mechanisms and genes involved in apoptosis. *Tumor Biol.* **2016**, *37*, 8471-8486, <https://doi.org/10.1007/s13277-016-5035-9>.
 45. Kaloni, D.; Diepstraten, S.T.; Strasser, A.; Kelly, G.L. BCL-2 protein family: attractive targets for cancer therapy. *Apoptosis* **2023**, *28*, 20-38, <https://doi.org/10.1007/s10495-022-01780-7>.
 46. Edlich, F. BCL-2 proteins and apoptosis: Recent insights and unknowns. *Biochem. Biophys. Res. Commun.* **2018**, *500*, 26-34, <https://doi.org/10.1016/j.bbrc.2017.06.190>.
 47. Campbell, K.J.; Tait, S.W.G. Targeting BCL-2 regulated apoptosis in cancer. *Open Biol.* **2018**, *8*, 180002, <https://doi.org/10.1098/rsob.180002>.